MOLEKUL
eISSN: 2503-0310

Articles
https://doi.org/10.20884/1.jm.2025.20.1.12063

Optimizing Dye-Sensitized Solar Cell Efficiency with a Triple Blend of *Caesalpinia sappan L., Dracaena angustifolia,* and *Clitoria ternatea L.*

Khofifatul Rahmawati[1], Nita Kusumawati[1,*], Pirim Setiarso[1], Supari Muslim[2], Nafisatus Zakiyah[1], Fadlurachman Faizal Fachrirakarsie[1]

[1]Department of Chemistry, Faculty of Mathematics and Natural Science, Universitas Negeri Surabaya, Surabaya, 60231, Indonesia
[2]Department of Electrical Engineering, Faculty of Engineering, Universitas Negeri Surabaya, Surabaya, 60231, Indonesia

*Corresponding author email: nitakusumawati@unesa.ac.id

Received June 04, 2024; **Accepted** December 30, 2024; **Available online** March 20, 2025

ABSTRACT. Dye-sensitized solar cells (DSSCs) offer a promising sustainable solution to global electricity challenges by converting sunlight into electricity using photosensitive dyes. This study explores the performance of DSSCs using natural dyes from sappanwood (*Caesalpinia sappan L.*), pandan leaves (*Dracaena angustifolia*), and telang flowers (*Clitoria ternatea L.*). Extraction of the dyes was done through maceration, with combinations made in single, double, and triple-component blends. UV-Vis spectroscopy showed increased light absorption in the 400-700 nm range. Combination F5 uniquely showed absorption peaks at 534.22, 573.64, 619.12, and 664.21 nm, which were affected by nine conjugated double bonds and electron transfer from C=C and carbonyl groups. Comparative band gap energy analysis showed that the triple-blending dyes exhibited the lowest energy range of 0.3392-0.4469 eV, compared to the double dye (0.4549-0.5778 eV) and single dye (0.4541-0.6248 eV), indicating better light harvesting ability. FTIR analysis confirmed the chemical structure of the dye. Prominent spectroscopic features include a broad band of 3332 cm^{-1} for hydroxyl groups, peaks at 2919 cm^{-1} and 1732 cm^{-1} representing alkane and carboxyl groups in cellulose, and an aromatic lignin C=C stretch at 1672 cm^{-1}. The optimized F5 blend (1:2:1 ratio) achieved the highest solar cell efficiency of 3.24% with a band gap of 0.3392 eV. These results validate the potential of natural dye blends as DSSC sensitizers, showing enhanced absorption spectrum, improved stability, and increased electric current generation.

Keywords: Dye-sensitized solar cells, Triple-component blending, *Caesalpinia sappan L., Dracaena angustifolia, Clitoria ternatea L.*

INTRODUCTION

Solar energy is a vital renewable energy source for life in a world where the global energy crisis increases the electricity demand, making it a major reason to focus on alternative renewable technology (Çakar, 2019; Kula et al., 2019; Yan et al., 2020). Solar energy is the most viable renewable source, given the enormous potential of solar radiation, estimated at 3.8 million exajoules per year, which exceeds global energy demand by about 15 TW per year (Kishore Kumar et al., 2020; Yahya et al., 2021). Every year, the issue of sourcing renewable energy becomes more and more relevant with the shift to environmentally friendly production (Ezhov et al., 2020). By 2050, 66% of the world's energy needs will come from renewable energy sources, which could reduce greenhouse gas emissions and the average global temperature rise by 2 °C (Enaganti et al., 2020). Solar energy, as a potential alternative, generates thermal energy for various applications due to the remarkable conversion effectiveness of the solar system into heat generated by one of the DSSCs (Said et al., 2023).

As a replacement for the utilization of solar cell technology, DSSCs are attracting much attention because they have sustainable advantages as an alternative to conventional-based solar cells with the benefits of low production costs, flexibility, and high power conversion efficiency, as well as no harmful effects on the environment (Dinesh et al., 2019; Jalali et al., 2020; Li et al., 2019; Mustafa et al., 2019; Wang et al., 2020). The basis of DSSCs is the idea that photosensitive dyes can generate electrical energy from solar energy. Glass substrates, transparent conductors, TiO_2 nanoparticles, electrolytes, counter electrodes, and natural dyes are some of the components of DSSCs (Weldemicheal et al., 2023).

The principle of DSSC operation involves sensor excitation, which causes the dye to oxidize by injecting electrons into the conduction band of the semiconductor. Thereafter, the excited electrons are

transferred to the carotenoid and diffused across the membrane, eventually being taken up by the electron acceptor (Omar et al., 2020; Vibavakumar et al., 2023). DSSC, as the third generation, uses natural dyes as a means of capturing light elements, where the entire transformation of solar cells into electricity occurs by DSSC components, including electron transport semiconductors, natural dyes as light absorbers, and electrolytes, where dye sensitivity determines the performance and efficiency of DSSC. DSSC is also affected by the total energy absorbed, where the energy is provided for the diffusion of electric current through photon energy, photoanodes, dye sensitizers, and electrodes (Mustafa et al., 2019; Semire et al., 2020; Shamsudin et al., 2023).

Dye sensitizer is one of the DSSC components that can be made from natural materials. An important component of a DSSC is the dye, which functions as an electron receiver when sunlight hits it. Natural dyes contain different coloring pigments, such as yellow (carotenoid pigments), green (chlorophyll pigments), and purple (anthocyanin pigments). The low stability of natural dyes and the fact that many of them do not have a very good anchoring site are the limits to the use of natural dyes in DSSC applications towards photoelectrodes, and their low efficiency (Y. Kusumawati et al., 2019). Although DSSCs with natural dyes have low efficiencies, we have experienced that developing dyes from leaves gives DSSCs higher efficiencies than roots (Chumwangwapee et al., 2023). Natural dyes are used in DSSCs due to their ability to absorb light, lower cost, environmentally friendly materials, design flexibility, and better efficiency. In this study, natural dyes were obtained from plant extracts such as sappanwood (*Caesalpinia sappan L.*), pandan leaves (*Dracaena angustifolia*), and telang flowers (*Clitoria ternatea L.*), which were then dyed with different extraction concentrations to obtain the absorption index indicating their light absorption ability. Several studies suggested different types of DSSC layers, such as the fabrication of different electrodes, electrolytes, conductive layers, and dyes as composite layers (Amir-Al Zumahi et al., 2021).

In this study, the fabrication of DSSCs with triple different natural dyes was studied by studying their optical behavior and analyzing the power conversion efficiency. These new dyes are expected to unlock the full discovery of DSSCs in the future through further research. The combination of these triple dyes can provide a wider range of light absorption, as each has a different absorption spectrum, thus potentially improving the efficiency of DSSCs. In this study, the fabrication of DSSCs using PVDF membrane as one of the hydrophobic polymers having good thermal stability, mechanical stability, and selective permeability in dye-sensitized solar cells (Pascariu et al., 2021; Zhang et al., 2021) and the utilization of PVDF membrane optimized by the electrospinning method, as well as the application of polymer matrix in polymer electrolyte in the operation of DSSCs with natural photosensitizers, have been studied. Although PVDF nanofiber (PVDF NF) electrolyte membranes have slightly decreased efficiency compared to liquid electrolytes, this study used these membranes due to their important stability advantages. The use of membrane-based electrolytes like PVDF-NF is a calculated decision that highlights the importance of improved stability in DSSC, as noted by (N. Kusumawati et al., 2023).

EXPERIMENTAL SECTION

Materials

The materials of this study included DMAc (N,N-Dimethylacetamide) (≥99.9% purity; Merck, Germany), PVDF (Poly(vinylidene fluoride)) (powder, Mw ~534,000; Sigma-Aldrich, France), Acetone (>99.5% purity; Sigma-Aldrich, Singapore), HNO_3 (≥99.9% pure; Sigma-Aldrich, Singapore), TiO_2 (≥99. 9% purity; Merck, Germany), anhydrous EC (99% purity; Merck, Germany), and Propylene carbonate (99.7% purity; Sigma-Aldrich, USA), PEG-1000 (Propylene glycol) (99% purity; Merck, Germany), KI (99% purity; Merck, Germany), Methanol (≥99. 7% purity; Merck, Germany), Tween 80 (≥99.8% purity; Smart-Lab, Indonesia), and Iodine (≥99.8%; Smart-Lab, Indonesia). FTO glass (resistivity 10 Ω) was produced by XinYu Xu Tking Glass Co,L in China. *Caesalpinia sappan L.*, *Dracaena angustifolia*, and *Clitoria ternatea L.* were purchased from local plantations (Surabaya, Indonesia).

Methods

The process of making organic photosensitizers through maceration follows the same approach as described in the research project conducted by (Estiningtyas et al., 2023). In this method, each natural dye, sappanwood (*C. sappan L.*), pandan leaves (*D. angustifolia*), and telang flowers (*C. ternatea L.*) obtained are then washed with water until clean. Then, after cleaning, each dye was extracted by maceration using methanol solvent in a ratio of 1:10 (sample: solvent) for 24 hours. The filtrate of each natural dye was then combined with a ratio of 50 mL. These three dyes were combined at various volume ratios to make various dye combinations.

TiO_2 Paste Formulation

The methodical preparation of TiO_2 paste was carried out according to a previously published protocol (Kusumawati et al., 2024). 0.8 g titanium oxide (TiO_2) and 0.32 g propylene glycol (PEG-1000) were mixed in this procedure. To achieve equal dispersion, the mixture was further enriched with 0.2 mL HNO_3 and 1.6 mL tween-80 while stirring vigorously for about 30 min at 100 rpm. Using the doctor blade method, the TiO_2 paste was then applied to the FTO anode with an active area of 3 cm^2. After one hour of sintering at 450 °C, the covered substrate produced clear products.

Table 1. The 12 dye combinations serve as sources of dye-sensitized solar cells

Type	Variation	Combination of Dye
Single	D1	100% yellow
	D2	100% green
	D3	100% purple
Double	E1	50% yellow + 50% green
	E2	50% green+ 50% purple
	E3	50% yellow + 50% purple
Triple	F1	60% yellow + 30% green + 10% purple
	F2	30% yellow + 10% green + 60% purple
	F3	10% yellow + 60% green + 30% purple
	F4	50% yellow + 25% green + 25% purple
	F5	25% yellow + 50% green + 25% purple
	F6	25% yellow + 25% green + 50% purple

Fabrication of PVDF Membrane

PVDF membranes were produced using the electrospinning technique, following the procedure established in a previous study by (Kusumawati et al., 2023).

Electrolyte Preparation

This electrolyte was made by following the procedure established by (Kusumawati et al., 2024). In the previous study, in the formulation process, 0.09 g of iodine (I2), 0.6 g of potassium iodide (KI), 4 g of propylene carbonate (PC), and 4 g of ethylene carbonate (EC) were carefully mixed through magnetic stirring at 100 rpm for one hour. A solution serving as the electrolyte was produced and then kept away from sunlight by storing it in a dark room to ensure optimal stability for subsequent applications.

Fabrication DSSC

After sintering, the TiO_2 photoanodes were subjected to immersion in a 10 mL solution of natural dye for 24 hours. Next, a precisely cut PVDF membrane, made through a combination of casting and electrospinning methods, was 2 cm long and 1.5 cm wide. The membrane was immersed in one milliliter of electrolyte. The conductive layer on the FTO glass substrate received a layer of wax-derived carbon. The DSSC circuit configuration was determined as FTO/TiO_2/PVDF/Pt/FTO.

Preparation of the working electrode was carried out by cleaning the FTO (fluorine-doped tin oxide) glass, applying TiO_2 paste (with the doctor blade technique), sintering at high temperature (450 °C), cooling, immersing in natural dye solution, and drying the electrode. The counter electrode preparation was done by FTO glass cleaning, platinum catalyst application, heat treatment, and cooling. Next, the PVDF membrane was immersed in the electrolyte solution. DSSC assembly is done by stacking the components (working electrode, electrolyte, counter electrode), clamping the edges, and a DSSC device is formed (**Figure 1**).

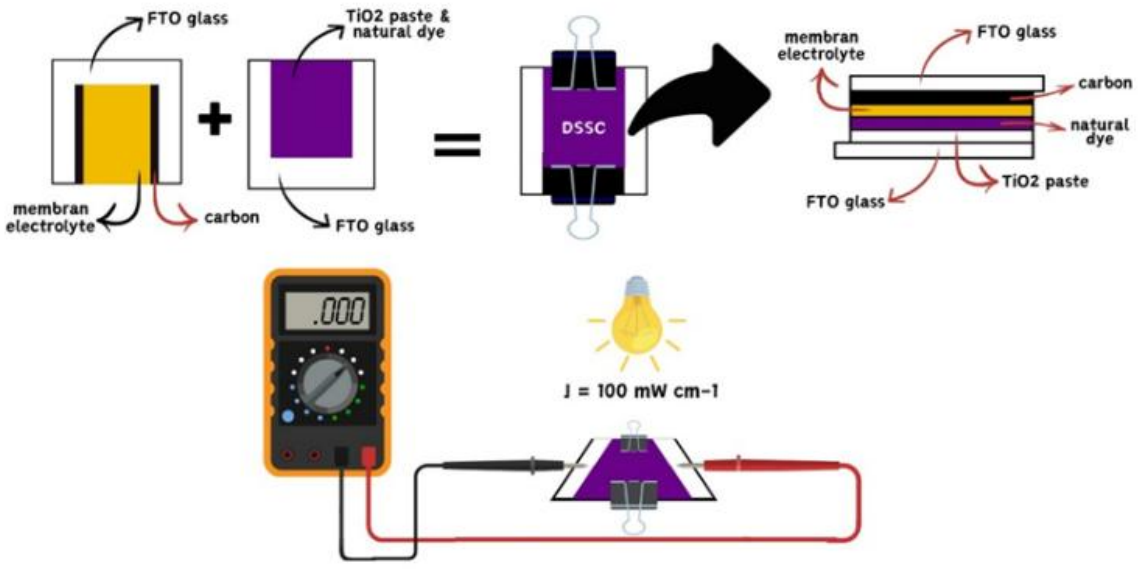

Figure 1. Schematic of the DSSCs sandwich

Characterization and Measurement for Photovoltaic Studies

The results of various combinations (single, double, and triple blending) using extracts from sappanwood (*C. sappan L.*), pandan leaves (*D. angustifolia*), and telang flowers (*C. ternatea L.*) were investigated. UV-Vis spectrophotometry was used to characterize the extracted chemicals. The amount of band gap energy was further determined by scanning at a rate of 20 mV/s over a potential range between -1 V and 1 V via the cyclic voltammetry (CV) technique. Characterization of the dye-sensitized solar cell (DSSC) includes fill factor (FF), efficiency, Voc, Isc, and Pin evaluation. A multimeter was used to measure the performance of the DSSC, while an LED light source with a brightness of 100 mW/cm^2 was used as the light source. The fill factor (FF) determines the overall cell performance, and the following formulas are used to calculate the fill factor (FF) equation (1) and efficiency (η) equation (2) (Maka & O'Donovan, 2022).

$$FF = \frac{Vmax \times I\,max}{Voc \times Isc} \quad (1)$$

$$\eta = \frac{FF \times Voc \times Isc}{Pin} \quad (2)$$

RESULTS AND DISCUSSION

UV-Visible Spectrum of Natural Dye

The dyes used in DSSCs play an important role in enhancing the assimilation of the visible light spectrum by TiO_2. Natural dyes offer important advantages compared to synthetic dyes due to their better accessibility, simplified extraction process with fewer chemical operations, high absorption coefficient, cost-effectiveness, non-toxicity, and biodegradability (Iman et al., 2024; Purushothamreddy et al., 2020). These natural colorants include pigments from various plants, including betalains, carotene, chlorophyll, and anthocyanins (Ammar et al., 2019; Oladeji et al., 2022). To determine the potential of sappanwood (*C. sappan L.*), pandan leaves (*D. angustifolia*), and telang flowers (*C. ternatea L.*) as natural dyes in DSSCs, testing was carried out using a UV-Vis spectrophotometer with visible light wavelengths between 400-750 nm (Estiningtyas et al., 2023).

This research significantly contributes to the understanding of the intricate characteristics that arise from the blending of sappanwood (yellow dye), pandan leaves (green dye), and telang flowers (purple dye) that are critical to their potential application as natural sensitizers in DSSCs. This investigation includes careful wavelength determination for each dye combination and offers important insights into the initial characterization of these blends. **Figure 2(a)** shows the highest absorption peaks for single dyes without blending sappanwood (yellow dye), pandan leaves (green dye), and telang flower (purple dye) covering the wavelength range of 400-750 nm, giving peak wavelengths for (D1) of 444.36 nm; for (D2) of 434.95 and 664.53 nm; and for (D3) of 532.78, 573.32, and 619.12 nm. Sappanwood, known as *C. sappan L.*, contains betalain pigments; these pigments are soluble in common polar solvents, including water. Sappanwood (*C. sappan L.*) contains an extract with the compound curcumin as its main yellow pigment. The main ingredient in sappan wood extract, curcumin, gives the material a clear yellow color (Sharifi-Rad et al., 2020). Experiments have shown that curcumin absorbs strongly at 350-470 nm. The absorption spectrum of curcumin, the main compound in sappanwood extract, has been carefully measured and found to cover the critical wavelength range of 350-470 nm. This explains its yellow color and provides details about its light-absorbing properties. Two absorption peaks were seen in *Pandanus amaryllifolius* chlorophyll at 434 and 664 nm, as stated in the study conducted by Ishak et al (Ishak* et al., 2019). Meanwhile, in telang flowers (*C. ternatea L.*), the absorption wavelength range is 500-700 nm (Tuan Putra et al., 2021).

Figure 2(b) shows the absorption properties of the sensitizer in the DSSC, where the synergistic effect of the double dye combination is seen. Specifically, the double blending of sappanwood and pandan leaves dyes designated as (E1), the combination of pandan leaves and telang dyes (E2), and the combination of sappanwood and telang dyes (E3) show different absorption peaks between 400 and 700 nm wavelengths. The specific peak wavelengths for these combinations were measured as follows: 440.21 and 664.61 nm for (E1); 573.64, 619.76, and 663.89 nm for (E2); and 574.28 and 620.48 nm for (E3). These results underscore the intricate interactions between natural dyes and illuminate their potential for applications in various wavelength-sensitive domains in DSSCs.

Meanwhile, in **Figure 2(c)**, the wavelength characteristics of the triple dyes, namely sappanwood, pandan leaves, and telang flower, are known to show the highest absorption peak in their combined composition. Analysis of the combined composition of these dyes showed the largest absorption peaks. This mixture was further adjusted in six different compositions (F1-F6), all of which were carefully measured in the wavelength range of 400-700 nm. When the three dyes were combined, they produced similar wavelengths showing three important peaks: 573, 619, and 664 nm. The specific peak wavelengths for this combination were measured as follows: for (F1) are 573.64, 619.12, and 664.61 nm; for (F2) are 441.89, 573.64, 619.12, and 664.61 nm; for (F3) were 613.70 and 664.21 nm; for (F4) were 573.64, 619.12, and 664.61 nm; for (F5) were 534.22, 573.64, 619.12, and 664.21 nm; and for (F6) were 40.53 and 664.61 nm. The absorption spectra in the wavelength range above 400 nm are affected by nine conjugated double bonds. The C=C conjugated double bond is responsible for the electron transfer from n to π^*, as shown in the 400-700 nm peak. Nine conjugated double bonds affect the absorption

spectrum in the wavelength range above 400 nm. On the other hand, the carbonyl group (C=O) is the source of electron transfer from n to π^* and is responsible for the peak at 430 nm (Rahmalia et al., 2021). The higher absorbance indicates that the triple-dye blend is more effective at absorbing light than a single dye; the greater cumulative absorption quality in the UV-Vis absorption spectrum demonstrates this. The triple-dye blend is more effective because it combines the unique light absorption capabilities of each dye, resulting in a more comprehensive system to absorb the light spectrum for solar cell applications. These results, which capture subtle differences in dye composition and corresponding optical characteristics, help clarify how these blends can be used as sensitizers in DSSCs and demonstrate their feasibility for use in solar energy conversion systems.

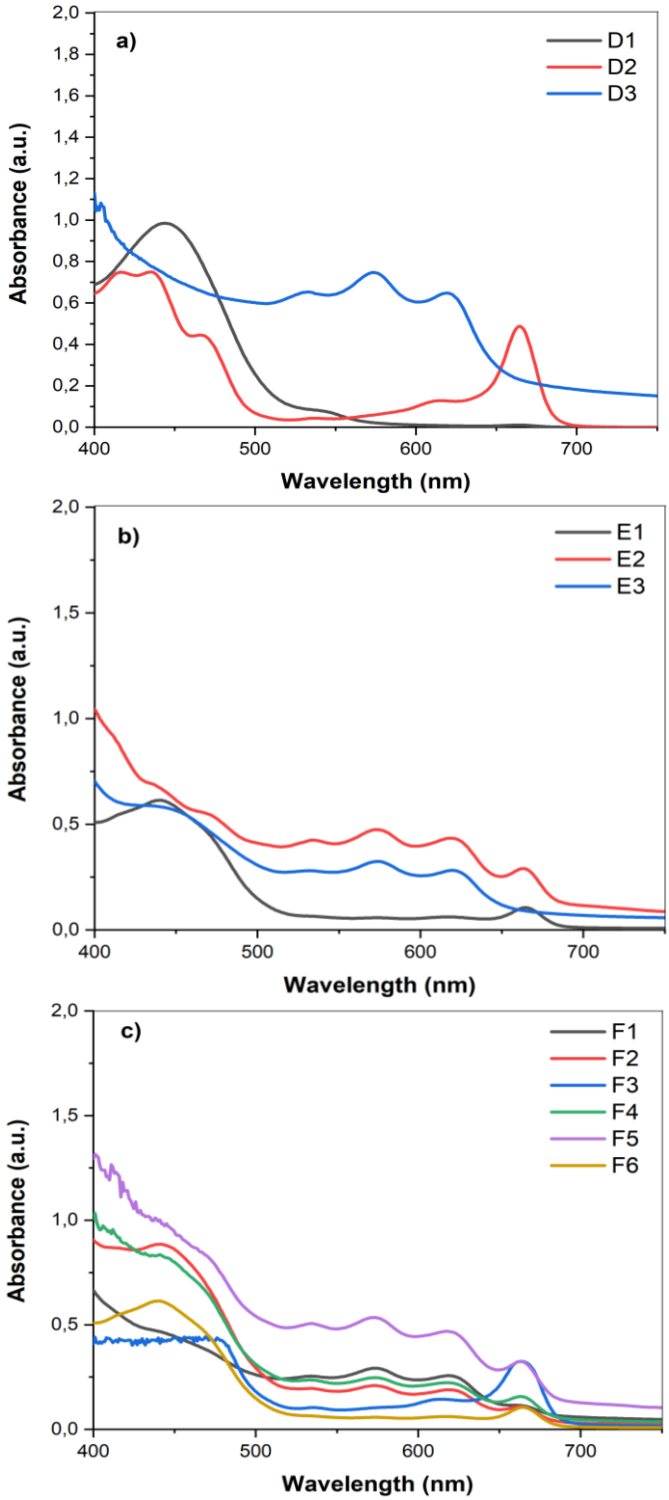

Figure 2. UV-Vis spectra of **a**) each single dye (red, yellow, and green), **b**) double blending of two dyes, and **c**) triple component blending of three dyes

FTIR Spectroscopy

FTIR analysis was performed to confirm the chemical structure of the extracted dye. In order for the absorption of natural dyes on the TiO_2 layer to take place effectively, the presence of special functional groups in the dye is required. In **Figure 3**, each dye (D1-F6) shows a broad band and peak appearing at wave number 3332 cm^{-1}, which indicates the presence of hydroxyl groups (O-H) in the fiber and water adsorption. This also indicates that cellulose, lignin, and water are contained in the fiber (Shaker et al., 2020). The presence of water in the fiber is proven through the water content test. Meanwhile, the absorption peaks at wave numbers 2919 cm^{-1} and 1732 cm^{-1} represent the stretching of alkane (C-H) and carboxyl (C=O) groups found in cellulose and hemicellulose (Hazrati et al., 2021). The C=C stretching of aromatic lignin was observed at 1672 cm^{-1}. In addition, the peak range of 1149-1414 cm^{-1} in the spectra of sapanwood, pandanus leaves, and telang flowers is related to stretch vibrations (C=O) of ester bonds of ferulate carboxyl groups and p-cumaric acid in hemicellulose and lignin (Ilyas et al., 2019). Cellulose polysaccharide constituents confirmed the presence of (C-O) and (O-H) stretching vibrations occurring at 1023 cm^{-1}. Through the FTIR analysis technique, it was confirmed that cellulose and hemicellulose are contained in the structural composition of the fiber.

The FTIR spectrum shows that the mixture of natural dyes from sappanwood, pandan leaves, and telang flowers did not produce new bonds. The blending of the three natural dyes can be seen in the FTIR spectrum; no reaction occurs with each other. This is similar to the research conducted by (Kabir et al., 2019a), which states that when these natural dyes are mixed, they will coexist peacefully and not react with each other.

Voltammetry Cyclic Analysis

The significance of the band gap lies in its contribution to the enhancement of photocatalytic activity, which is manifested through increased electron transfer capability, increased light harvesting capability, and increased catalytic active sites (Ahmad et al., 2023). The amount of band gap energy for each dye has been calculated using the cyclic voltammetry (CV) technique. The value of this important energy parameter is obtained by examining the difference between the Highest Occupied Molecular Orbital (HOMO) and the Lowest Unoccupied Molecular Orbital (LUMO) (Dejpasand et al., 2020). Specifically, in CV analysis, the oxidation state is denoted by the oxidation peak for HOMO values, and the reduction peak indicates the reduction state for LUMO values. Equations (3-5) are used to determine the band gap energy, HOMO, and LUMO values (Setiarso et al., 2023).

$$E_{HOMO} = -(E_{ox} + 4.40)\ eV \quad (3)$$

$$E_{LUMO} = -e\ (E_{red} + 4.40)\ eV \quad (4)$$

$$Eg = E_{LUMO} - E_{HOMO} \quad (5)$$

Based on **Table 3**, the energy band gap values obtained for each dye with various compositions indicate that the triple component blending pigments from (*C. sappan L.*), pandan leaves (*D. angustifolia*), and telang flowers (*C. ternatea L.*) can be used as natural dyes/sensitizers in DSSCs because they meet the requirements as DSSC dyes. The LUMO value of each dye is significantly greater than the conduction value of TiO_2. The dye must meet the requirement of having a sufficiently high LUMO level compared to the -4.0 eV conduction band of the TiO_2 semiconductor, which guarantees the capacity of the semiconductor to accept electron injection from the excited dye (Elroby et al., 2023; Olusegun et al., 2021).

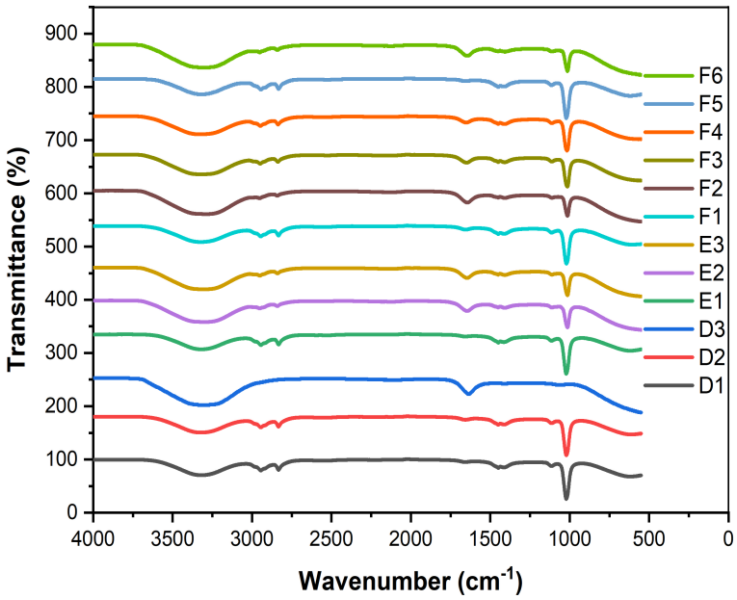

Figure 3. Spectra FTIR of each single dye (D1–D3), double blending of two dyes (E1–E3), and triple component blending of three dyes (F1–F6)

Table 3. Values of the band gap, HOMO, and LUMO for each potential dye combination

Dye (Various compositions)		HOMO (eV)	LUMO (eV)	Band Gap Energy (eV)
D	(1) 1:0:0	-4.2862	-3.6614	0.6248
	(2) 0:1:0	-4.2663	-3.6669	0.5994
	(3) 0:0:1	-4.5009	-4.0468	0.4541
E	(1) 1:1:0	-4.1099	-3.5528	0.5571
	(2) 0:1:1	-4.0437	-3.4659	0.5778
	(3) 1:0:1	-4.1267	-3.6718	0.4549
F	(1) 6:3:1	-4.0636	-3.6184	0.4452
	(2) 3:1:6	-3.9966	-3.5497	0.4469
	(3) 1:6:3	-4.1402	-3.7484	0.3918
	(4) 2:1:1	-4.1003	-3.7611	0.3392
	(5) 1:2:1	-4.1769	-3.8147	0.3622
	(6) 1:1:2	-4.0141	-3.5784	0.4357

This makes it possible to regulate the LUMO dye energy so that, when the semiconductor surface is exposed to electron injection, there is enough driving force to allow the dye regeneration process to occur in the DSSC (Kabir et al., 2019b).

Table 3 shows that each dye combination has an energy gap between 0.3392 eV and 0.6248 eV. Notably, the triple-component blending shows the smallest energy gap, followed by the double-component blending and the single dye without blending. The specific composition variation F5 (1:2:1) has the most favorable energy gap in this study with a band gap value of 0.3392 eV. A reduced band gap implies a narrower energy difference between the conduction band and the valence band, facilitating electron movement and thus increasing electrical conductivity (Estiningtyas et al., 2023). The lower HOMO-LUMO energy gap promotes a shift towards absorption spectra with longer wavelengths, known as a bathochromic shift, which is favorable for improving the efficiency of photovoltaic devices.

Photovoltaic Studies

Dyes have a significant function in absorbing and converting light into electrical energy. Thus, the performance of dye-sensitized solar cells (DSSCs) is strongly influenced by the type of dye used as a sensitizer material. Some of the factors that determine dye selection include the spectrum of light absorption by the dye, the mass of active electrons, the ability to transfer charge from dye to TiO_2, and the mechanism of dye binding to the TiO_2 surface (Omar et al., 2020). Dye variations in DSSC produce several photovoltaic parameters. The final calculation of these parameters is the performance efficiency of the DSSC, which greatly affects its potential as an environmentally friendly alternative energy. Dye variation in DSSC produces photovoltaic parameters. The final calculation result of the Voc, Isc, and FF parameters is the performance efficiency of the DSSC, which greatly affects its potential as an environmentally friendly alternative energy source. The efficiency is strongly influenced by the dye used. Then, the J-V curve is generated through the photovoltaic parameters that have been generated. The resulting curvature states the performance efficiency possessed by each sample.

In **Table 4**, presenting single dyes in D(1), D(2), and D(3), which are explicitly described in **Figure 4(a)**, yields efficiencies of 0.61%, 0.97%, and 1.69%. Double-blending dyes yielded higher values for E(1), E(2), and E(3) with values of 1.87%, 2.24%, and 2.12%. The difference in these values is explained in **Figure 4(b)**. The significant increase that occurred in E(2) and E(3) was due to the influence of telang flower (*C. ternatea L.*), which had the best efficiency value. Telang flowers provide an increase in efficiency due to their broad absorption characteristics, good interaction with TiO_2, and color absorption stability, which overall contribute to the improved performance of DSSCs. Junger et al. (2019) explained that the absorption rate of striped flowers affects the interaction between the dye and the TiO_2 surface (Juhász Junger et al., 2019). Extraction temperature, solvent, and pH of the dye solution are some of the variables that affect this interaction. DSSC efficiency is also affected by the overlap of the dye absorption spectrum and the luminance spectrum. The overlap of the dye absorption spectrum and its match with the illumination spectrum is critical as it affects the ability of the DSSC to absorb and convert light into electrical energy, which ultimately determines the overall system efficiency. Zakar et al. (2021) added that this broad absorption can also provide optimal DSSC performance efficiency due to the stability of color absorption (Zakar et al., 2021).

Table 4. Photovoltaic Parameters of the DSSC

Dye (Various compositions)		Voc (mV)	Isc (mA/cm^2)	FF (%)	Efficiency (%)
D	(1) 1:0:0	226	0.0023	0.348	0.61
	(2) 0:1:0	287	0.0025	0.405	0.97
	(3) 0:0:1	362	0.0029	0.483	1.69
E	(1) 1:1:0	375	0.0030	0.499	1.87
	(2) 0:1:1	423	0.0033	0.480	2.24
	(3) 1:0:1	399	0.0031	0.515	2.12
F	(1) 6:3:1	435	0.0034	0.495	2.44
	(2) 3:1:6	428	0.0033	0.482	2.27
	(3) 1:6:3	461	0.0035	0.510	2.74
	(4) 2:1:1	504	0.0036	0.526	3.18
	(5) 1:2:1	513	0.0037	0.512	3.24
	(6) 1:1:2	441	0.0034	0.496	2.48

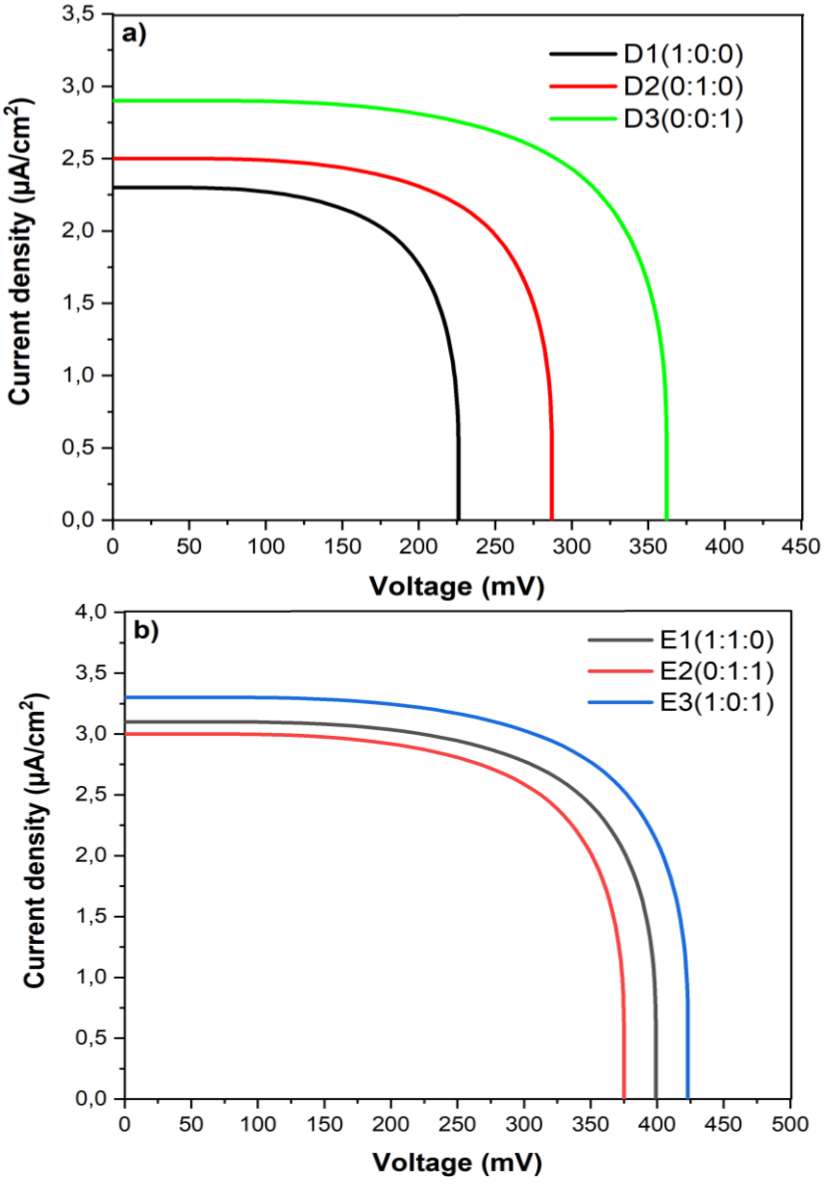

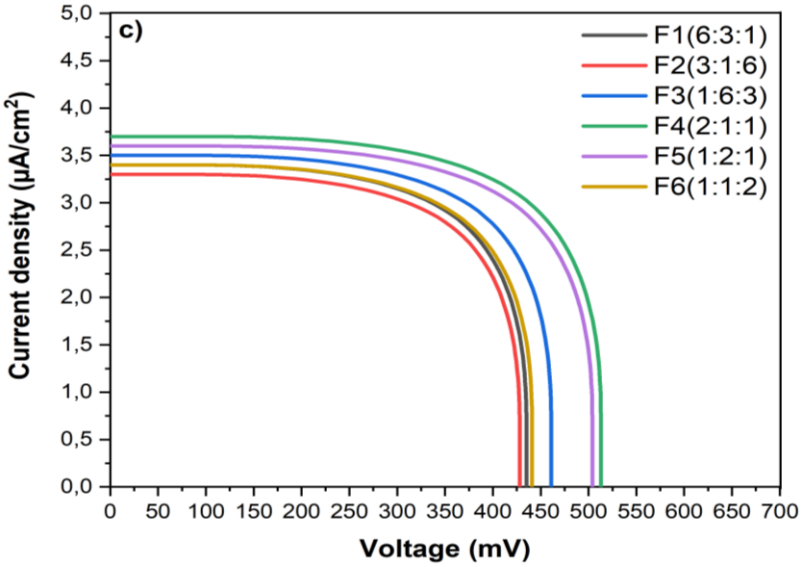

Figure 4. Photocurrent-voltage curves were obtained for DSSC sensitized of a) each single dye (yellow, green, and purple), b) double blending of two dyes, and c) triple component blending of three dyes

The results in **Table 4** are further supported by the scientific findings that the wavelength absorption is expanded by triple blending the dyes. The J-V curve shown in **Figure 4(c)** explains that triple blending of dyes in DSSC can significantly affect its efficiency. This can be seen in samples F(1-6), where the efficiency of DSSC performance increases with values of 2.44%, 2.27%, 2.74%, 3.18%, 3.24%, and 2.48%. This is still dominated by a large concentration of pandan leaves so as to produce the highest performance efficiency compared to other samples. Kabir et al. (2019b) explained that an appropriate dye mixture ratio can improve the absorption and adsorption properties of the dye, leading to an increase in performance efficiency (Kabir et al., 2019a). This was further supported by Zhang et al. (2020), who showed that dyes with longer hydrocarbon chains can improve the efficiency of DSSCs due to higher molar absorption coefficients (Zhang et al., 2020). Mcyotto et al. (2021) also highlighted the importance of dye structure, with certain configurations leading to improved performance (Mcyotto et al., 2021). Junger et al. (2019) emphasized the role of the color spectrum in the efficiency of DSSCs, pointing out that dye selection must be precise (Juhász Junger et al., 2019). Thus, color absorption will occur optimally.

The most successful triple-component blending combination was F5 (1:2:1) out of twelve different dye combinations examined. The efficiency ranking was F (triple-component blending) > E (double-component blending) > D (no blending). Voc, Isc, FF, and photoconversion efficiency of dye F5 were 513 mV, 0.0037 mA/cm^2, 0.512%, and 3.24%, respectively. The F5 (1:2:1) dye has a narrower band gap, in agreement with this alignment with previous band gap studies. Since there are more conjugated chains, a smaller band gap value indicates faster electron transmission (Tractz et al., 2019). The F5 (1:2:1) dye has the shortest band gap across the composition variants, according to the band gap data, which is attributed to improved performance explained by better absorption of sunlight and more effective use of photon energy (Zhou et al., 2021).

CONCLUSIONS

This study shows that natural dyes from sappanwood (*C. sappan L.*), pandan leaves (*D. angustifolia*), and telang flowers (*C. ternatea L.*) have promising potential as sensitizers in dye-sensitized solar cells (DSSCs). UV-visible spectrum analysis confirmed that the triple dyes produced optimal uptake with three main peaks at 573, 619, and 664 nm. FTIR analysis confirmed the chemical structure of the natural dyes, showing a broad band at 3332 cm^{-1} indicating the presence of hydroxyl (O-H) groups and absorption peaks at 2919 cm^{-1} and 1732 cm^{-1} representing alkane stretching (C-H) and carboxyl (C=O) groups in cellulose and hemicellulose. C=C stretching of aromatic lignin is observed at 1672 cm^{-1}, while the peak range of 1149-1414 cm^{-1} is related to C=O stretching vibrations of ester bonds. The polysaccharide component of cellulose was confirmed through C—O and O—H stretching vibrations at 1023 cm^{-1}. FTIR analysis proved that the dyes could blend without forming new bonds. Through cyclic voltammetry analysis, it was found that the optimal composition of F5 (1:2:1) showed the lowest energy band gap of 0.3392 eV, with a LUMO value suitable for DSSC applications. The photovoltaic performance showed a significant increase in efficiency from single dye (0.61-1.69%) to double dye blending (1.87-2.24%) to triple dye blending (2.27-3.24%), with the highest efficiency of 3.24% achieved at composition F5 (1:2:1), which resulted in Voc 513 mV, Isc 0.0037 mA/cm^2, and FF 0.512%. These results confirm that triple blending natural dyes with an optimal

composition can significantly improve the performance of DSSCs, providing an environmentally friendly and potential alternative for the development of solar cell technology in the future..

ACKNOWLEDGMENTS

The author acknowledges the financial support provided by the Indonesian Ministry of Education, Culture, Research, and Technology through national competitive research grants.

REFERENCES

Ahmad, I., Zou, Y., Yan, J., Liu, Y., Shukrullah, S., Naz, M. Y., Hussain, H., Khan, W. Q., & Khalid, N. R. (2023). Semiconductor photocatalysts: A critical review highlighting the various strategies to boost the photocatalytic performances for diverse applications. *Advances in Colloid and Interface Science*, *311*(November 2022). https://doi.org/10.1016/j.cis.2022.102830

Amir-Al Zumahi, S. M., Arobi, N., Mahbubur Rahman, M., Kamal Hossain, M., Ara Jahan Rozy, M., Bashar, M. S., Amri, A., Kabir, H., Abul Hossain, M., & Ahmed, F. (2021). Understanding the optical behaviours and the power conversion efficiency of novel organic dye and nanostructured TiO2-based integrated DSSCs. *Solar Energy*, *225*(July), 129–147. https://doi.org/10.1016/j.solener.2021.07.024

Ammar, A. M., Mohamed, H. S. H., Yousef, M. M. K., Abdel-Hafez, G. M., Hassanien, A. S., & Khalil, A. S. G. (2019). Dye-Sensitized Solar Cells (DSSCs) based on extracted natural dyes. *Journal of Nanomaterials*, *2019*. https://doi.org/10.1155/2019/1867271

Çakar, S. (2019). 1,10 phenanthroline 5,6 diol metal complex (Cu, Fe) sensitized solar cells: A cocktail dye effect. *Journal of Power Sources*, *435*(June), 226825. https://doi.org/10.1016/j.jpowsour.2019.226825

Chumwangwapee, N., Suksri, A., & Wongwuttanasatian, T. (2023). Investigation of bi-colour natural dyes potential for dye sensitized solar cell. *Energy Reports*, *9*, 415–421. https://doi.org/10.1016/j.egyr.2023.05.132

Dejpasand, M. T., Saievar-Iranizad, E., Bayat, A., Montaghemi, A., & Ardekani, S. R. (2020). Tuning HOMO and LUMO of three region (UV, Vis and IR) photoluminescent nitrogen doped graphene quantum dots for photodegradation of methylene blue. *Materials Research Bulletin*, *128*(February). https://doi.org/10.1016/j.materresbull.2020.110886

Dinesh, V. P., Sriram kumar, R., Sukhananazerin, A., Mary Sneha, J., Manoj Kumar, P., & Biji, P. (2019). Novel stainless steel based, eco-friendly dye-sensitized solar cells using electrospun porous ZnO nanofibers. *Nano-Structures and Nano-Objects*, *19*, 100311. https://doi.org/10.1016/j.nanoso.2019.100311

Elroby, S. A. K., Bouzzine, S. M., Al-Ghamdi, H. A., Alotaibi, M. M., & El-Shishtawy, R. M. (2023). Molecular understanding of electron donor influences in dye-sensitized solar cells of novel series-based D-A′-(π-A)2. *Materials Science in Semiconductor Processing*, *165*(June). https://doi.org/10.1016/j.mssp.2023.107675

Enaganti, P. K., Dwivedi, P. K., Srivastava, A. K., & Goel, S. (2020). Analysis of submerged amorphous, mono-and poly-crystalline silicon solar cells using halogen lamp and comparison with xenon solar simulator. *Solar Energy*, *211*(May), 744–752. https://doi.org/10.1016/j.solener.2020.10.025

Estiningtyas, I. W., Kusumawati, N., Setiarso, P., Muslim, S., Rahayu, N. T., Safitri, R. N., Zakiyah, N., & Fachrirakarsie, F. F. (2023). Effect of natural dye combination and pH extraction on the performance of dye-sensitized photovoltaics solar cell. *International Journal of Renewable Energy Development*, *12*(6), 1054–1060. https://doi.org/10.14710/ijred.2023.56172

Ezhov, A. V., Aleksandrov, A. E., Zhdanova, K. A., Zhdanov, A. P., Klyukin, I. N., Zhizhin, K. Y., Bragina, N. A., Mironov, A. F., & Tameev, A. R. (2020). Synthesis of Zn(II) porphyrin dyes and revealing an influence of their alkyl substituents on performance of dye-sensitized solar cells. *Synthetic Metals*, *269*(July), 116567. https://doi.org/10.1016/j.synthmet.2020.116567

Hazrati, K. Z., Sapuan, S. M., Zuhri, M. Y. M., & Jumaidin, R. (2021). Extraction and characterization of potential biodegradable materials based on dioscorea hispida tubers. *Polymers*, *13*(4), 1–19. https://doi.org/10.3390/polym13040584

Ilyas, R. A., Sapuan, S. M., Ibrahim, R., Abral, H., Ishak, M. R., Zainudin, E. S., Asrofi, M., Atikah, M. S. N., Huzaifah, M. R. M., Radzi, A. M., Azammi, A. M. N., Shaharuzaman, M. A., Nurazzi, N. M., Syafri, E., Sari, N. H., Norrrahim, M. N. F., & Jumaidin, R. (2019). Sugar palm (Arenga pinnata (Wurmb.) Merr) cellulosic fibre hierarchy: A comprehensive approach from macro to nano scale. *Journal of Materials Research and Technology*, *8*(3), 2753–2766. https://doi.org/10.1016/j.jmrt.2019.04.011

Iman, R. N., Harrabi, K., Younas, M., & Mekki, A. (2024). Fabrication of efficient natural dye-sensitized Solar Cells using Mediterranean olive leaves as natural dye sensitizer. *Journal of Photochemistry and Photobiology A: Chemistry*, *450*(January). https://doi.org/10.1016/j.jphotochem.2024.115477

Ishak*, N., Salleh, H., Dagang, A. N., Salisa, A. R., Kamarulzaman, N. H., Ghazali, S. M., Majid, N. A., & Ahmad, Z. (2019). Hybrid solar cell using conjugated chlorophyll from pandanus amaryllifolius as photosensitizers. *International Journal of Recent Technology and Engineering (IJRTE)*, *8*(4), 10142–10147. https://doi.org/10.35940/ijrte.d4361.118419

Jalali, T., Arkian, P., Golshan, M., Jalali, M., & Osfouri, S. (2020). Performance evaluation of natural native dyes as photosensitizer in dye-sensitized solar cells. *Optical Materials*, *110*(July), 110441. https://doi.org/10.1016/j.optmat.2020.110441

Juhász junger, I., Werner, D., Schwenzfeier-Hellkamp, E., & Ehrmann, A. (2019). Influence of illumination spectra on DSSC performance. *Optik*, *177*(September 2018), 8–12. https://doi.org/10.1016/j.ijleo.2018.09.123

Kabir, F., Bhuiyan, M. M. H., Hossain, M. R., Bashar, H., Rahaman, M. S., Manir, M. S., Ullah, S. M., Uddin, S. S., Mollah, M. Z. I., Khan, R. A., Huque, S., & Khan, M. A. (2019a). Improvement of efficiency of Dye Sensitized Solar Cells by optimizing the combination ratio of Natural Red and Yellow dyes. *Optik*, *179*(July 2018), 252–258. https://doi.org/10.1016/j.ijleo.2018.10.150

Kabir, F., Bhuiyan, M. M. H., Hossain, M. R., Bashar, H., Rahaman, M. S., Manir, M. S., Ullah, S. M., Uddin, S. S., Mollah, M. Z. I., Khan, R. A., Huque, S., & Khan, M. A. (2019b). Improvement of efficiency of Dye Sensitized Solar Cells by optimizing the combination ratio of Natural Red and Yellow dyes. *Optik*, *179*(September 2018), 252–258. https://doi.org/10.1016/j.ijleo.2018.10.150

Kumar, K. D., Kříž, J., Bennett, N., Chen, B., Upadhayaya, H., Reddy, K. R., & Sadhu, V. (2020). Functionalized metal oxide nanoparticles for efficient dye-sensitized solar cells (DSSCs): A review. *Materials Science for Energy Technologies*, *3*, 472–481. https://doi.org/10.1016/j.mset.2020.03.003

Kula, S., Szlapa-Kula, A., Fabiańczyk, A., Gnida, P., Libera, M., Bujak, K., Siwy, M., & Schab-Balcerzak, E. (2019). Effect of thienyl units in cyanoacrylic acid derivatives toward dye-sensitized solar cells. *Journal of Photochemistry and Photobiology B: Biology*, *197*(July), 111555. https://doi.org/10.1016/j.jphotobiol.2019.111555

Kusumawati, N., Setiarso, P., Muslim, S., Hafidha, Q. A., Cahyani, S. A., & Fachrirakarsie, F. F. (2024). Optimization Thickness of Photoanode Layer and Membrane as Electrolyte Trapping Medium for Improvement Dye-Sensitized Solar Cell Performance. *Science and Technology Indonesia*, *9*(1), 7–16. https://doi.org/10.26554/sti.2024.9.1.7-16

Kusumawati, N., Setiarso, P., Santoso, A. B., Muslim, S., A'yun, Q., & Putri, M. M. (2023). Characterization of Poly(vinylidene fluoride) nanofiber-based electrolyte and its application to dye-sensitized solar cell with natural dyes. *Indonesian Journal of Chemistry*, *23*(1), 113. https://doi.org/10.22146/ijc.75357

Kusumawati, Y., Oktavianti, I., N., Oktavia, W., L., Widiastuti, N., Atmaja, L.., Abu Bakar, I. N., & Hadi, N. (2019). Combined computational and experimental study the effect of doped magnesium into betanine-sensitized tio2 photoanode for dye-sensitized solar cells application. *Indonesian Journal of Chemistry*, *19*(4), 892–899. https://doi.org/10.22146/ijc.36861

Li, W., Ren, W., Chen, Z., Lu, T. F., Deng, L., Tang, J., Zhang, X., Wang, L., & Bai, F. Q. (2019). Theoretical design of porphyrin dyes with electron-deficit heterocycles towards near-IR light sensitization in dye-sensitized solar cells. *Solar Energy*, *188*(June), 742–749. https://doi.org/10.1016/j.solener.2019.06.062

Maka, A. O. M., & O'Donovan, T. S. (2022). Effect of thermal load on performance parameters of solar concentrating photovoltaic: High-efficiency solar cells. *Energy and Built Environment*, *3*(2), 201–209. https://doi.org/10.1016/j.enbenv.2021.01.004

Mcyotto, F., Wei, Q., Macharia, D. K., Huang, M., Shen, C., & Chow, C. W. K. (2021). Effect of dye structure on color removal efficiency by coagulation. *Chemical Engineering Journal*, *405*(August 2020). https://doi.org/10.1016/j.cej.2020.126674

Mustafa, M. N., Shafie, S., Wahid, M. H., & Sulaiman, Y. (2019). Optimization of power conversion efficiency of polyvinyl-alcohol/titanium dioxide as light scattering layer in DSSC using response surface methodology/central composite design. *Results in Physics*, *15*(August). https://doi.org/10.1016/j.rinp.2019.102559

Oladeji, O. S., Ikhile, M. I., Mamo, M., Ndinteh, D. T., & Ndungu, P. G. (2022). Extraction, characterization and energy investigation of Garcinia kola, Cola Nitida and Cola Accuminata for efficient light absorption in dye-sensitized solar cells. *Solar Energy*, *244*(September), 386–400. https://doi.org/10.1016/j.solener.2022.08.053

Olusegun, S., Semire, B., & Abidemi, M. (2021). Heliyon organic dyes for dye-sensitized solar cells . DFT / TDDFT investigations. *Heliyon*, *7*(December 2020), e06827. https://doi.org/10.1016/j.heliyon.2021.e06827

Omar, A., Ali, M. S., & Abd Rahim, N. (2020). Electron transport properties analysis of titanium dioxide dye-sensitized solar cells (TiO2-DSSCs) based

natural dyes using electrochemical impedance spectroscopy concept: A review. *Solar Energy*, *207*(July), 1088–1121. https://doi.org/10.1016/j.solener.2020.07.028

Pascariu, P., Cojocaru, C., Samoila, P., Olaru, N., Bele, A., & Airinei, A. (2021). Novel electrospun membranes based on PVDF fibers embedding lanthanide doped ZnO for adsorption and photocatalytic degradation of dye organic pollutants. *Materials Research Bulletin*, *141*(January), 111376. https://doi.org/10.1016/j.materresbull.2021.111376

Purushothamreddy, N., Dileep, R. K., Veerappan, G., Kovendhan, M., & Joseph, D. P. (2020). Prickly pear fruit extract as photosensitizer for dye-sensitized solar cell. *Spectrochimica Acta - Part A: Molecular and Biomolecular Spectroscopy*, *228*. https://doi.org/10.1016/j.saa.2019.117686

Rahmalia, W., Septiani, Naselia, U. A., Usman, T., Silalahi, I. H., & Mouloungui, Z. (2021). Performance improvements of bixin and metal-bixin complexes sensitized solar cells by 1-methyl-3-propylimidazolium iodide in electrolyte system. *Indonesian Journal of Chemistry*, *21*(3), 669–678. https://doi.org/10.22146/ijc.60633

Said, Z., Sohail, M. A., Pandey, A. K., Sharma, P., Waqas, A., Chen, W. H., Nguyen, P. Q. P., Nguyen, V. N., Pham, N. D. K., & Nguyen, X. P. (2023). Nanotechnology-integrated phase change material and nanofluids for solar applications as a potential approach for clean energy strategies: Progress, challenges, and opportunities. *Journal of Cleaner Production*, *416*(March). https://doi.org/10.1016/j.jclepro.2023.137736

Semire, B., Oyebamiji, A. K., & Odunola, O. A. (2020). Electronic properties' modulation of D–A–A via fluorination of 2-cyano-2-pyran-4-ylidene-acetic acid acceptor unit for efficient DSSCs: DFT-TDDFT approach. *Scientific African*, *7*, e00287. https://doi.org/10.1016/j.sciaf.2020.e00287

Setiarso, P., Harsono, R. V., & Kusumawati, N. (2023). Fabrication of Dye Sensitized Solar Cell (DSSC) Using Combination of Dyes Extracted from Curcuma (Curcuma xanthorrhiza) Rhizome and Binahong (Anredera cordifolia) Leaf with Treatment in pH of the Extraction. *Indonesian Journal of Chemistry*, *23*(4), 924–936. https://doi.org/10.22146/ijc.77860

Shaker, K., Waseem Ullah Khan, R. M., Jabbar, M., Umair, M., Tariq, A., Kashif, M., & Nawab, Y. (2020). Extraction and characterization of novel fibers from Vernonia elaeagnifolia as a potential textile fiber. *Industrial Crops and Products*, *152*(April 2019), 112518. https://doi.org/10.1016/j.indcrop.2020.112518

Shamsudin, N. H., Shafie, S., Ab Kadir, M. Z. A., Ahmad, F., Sulaiman, Y., Chachuli, S. A. M., & Razali, M. C. (2023). Flexible back-illuminated dye sensitised solar cells (DSSCs) with titanium dioxide/silver nanoparticles composite photoanode for improvement of power conversion efficiency. *Optik*, *272*(August 2022). https://doi.org/10.1016/j.ijleo.2022.170237

Sharifi-Rad, J., Rayess, Y. El, Rizk, A. A., Sadaka, C., Zgheib, R., Zam, W., Sestito, S., Rapposelli, S., Neffe-Skocińska, K., Zielińska, D., Salehi, B., Setzer, W. N., Dosoky, N. S., Taheri, Y., El Beyrouthy, M., Martorell, M., Ostrander, E. A., Suleria, H. A. R., Cho, W. C., … Martins, N. (2020). Turmeric and Its Major Compound Curcumin on Health: Bioactive Effects and Safety Profiles for Food, Pharmaceutical, Biotechnological and Medicinal Applications. *Frontiers in Pharmacology*, *11*(September), 1–23. https://doi.org/10.3389/fphar.2020.01021

Tractz, G. T., Viomar, A., Dias, B. V., De Lima, C. A., Banczek, E. P., Da Cunha, M. T., Antunes, S. R. M., & Rodrigues, P. R. P. (2019). Recombination study of dye sensitized solar cells with natural extracts. *Journal of the Brazilian Chemical Society*, *30*(2), 371–378. https://doi.org/10.21577/0103-5053.20180186

Tuan Putra, T. N. M., Zainol, M. K., MohdIsa, N. S., & MohdMaidin, N. (2021). Chemical characterization of ethanolic extract of Butterfly pea flower (Clitoria ternatea). *Food Research*, *5*(4), 127–134. https://doi.org/10.26656/fr.2017.5(4).744

Vibavakumar, S., Nisha, K. D., Manikandan, V. S., Archana, J., Navaneethan, M., & Harish, S. (2023). Enhanced photo conversion efficiency of Nb2O5/TiO2 bilayer photoanode for Dye-Sensitized Solar Cells. *Optical Materials*, *140*(April), 1–7. https://doi.org/10.1016/j.optmat.2023.113828

Wang, X., Bolag, A., Yun, W., Du, Y., Eerdun, C., Zhang, X., Bao, T., Ning, J., Alata, H., & Ojiyed, T. (2020). Enhanced performance of dye-sensitized solar cells based on a dual anchored diphenylpyranylidene dye and N719 co-sensitization. *Journal of Molecular Structure*, *1206*, 127694. https://doi.org/10.1016/j.molstruc.2020.127694

Weldemicheal, H. T., Desta, M. A., & Mekonnen, Y. S. (2023). Derivatized photosensitizer for an improved performance of the dye-sensitized solar cell. *Results in Chemistry*, *5*(October 2022). https://doi.org/10.1016/j.rechem.2023.100838

Yahya, M., Bouziani, A., Ocak, C., Seferoğlu, Z., & Sillanpää, M. (2021). Organic/metal-organic photosensitizers for dye-sensitized solar cells

(DSSC): Recent developments, new trends, and future perceptions. *Dyes and Pigments*, *192*(January). https://doi.org/10.1016/j.dyepig.2021.109227

Yan, C., Qu, M., Chen, Y., & Feng, M. (2020). Snow removal method for self-heating of photovoltaic panels and its feasibility study. *Solar Energy*, *206*(April), 374–380. https://doi.org/10.1016/j.solener.2020.04.064

Zakar, A. M. A., Naman, S. A., & Ahmed, S. M. (2021). Evaluation of the suitability of natural flower dyes spectra on dye-sensitized solar cell (DSSC) Containing TiO2and I-/I-3with respect to stability and efficiency. *IEEE Journal of Photovoltaics*, *11*(3), 838–846. https://doi.org/10.1109/JPHOTOV.2021.3063017

Zhang, H., Chen, Z. E., & Tian, H. R. (2020). Molecular engineering of metal-free organic sensitizers with polycyclic benzenoid hydrocarbon donor for DSSC applications: The effect of the conjugate mode. *Solar Energy*, *198*(October 2019), 239–246. https://doi.org/10.1016/j.solener.2020.01.067

Zhang, L., Shi, X., Zhao, M., Yin, Z., Zhang, J., Wang, S., Du, W., Xiang, J., Cheng, P., & Tang, N. (2021). Construction of precisely controllable and stable interface bonding Au-TiO2/PVDF composited membrane for biofouling-resistant properties. *Surfaces and Interfaces*, *24*(February), 101152. https://doi.org/10.1016/j.surfin.2021.101152

Zhou, P., Lin, B., Chen, R., An, Z., Chen, X., An, Q., & Chen, P. (2021). Effect of Extending the Conjugation of Dye Molecules on the Efficiency and Stability of Dye-Sensitized Solar Cells. *ACS Omega*, *6*(44), 30069–30077. https://doi.org/10.1021/acsomega.1c04794